Title: Spatio-temporal expression of TRPM4 in the mouse cochlea

Short running title: Expression of TRPM4 in the mouse cochlea

Author names and affiliations: Mayumi Sakuraba[1], Junko Murata[1], Ryoichi Teruyama[2], Kazusaku Kamiya[1], Junji Yamaguchi[3], Hideyuki Okano[4], Yasuo Uchiyama[3], Katsuhisa Ikeda[1]

[1]Department of Otorhinolaryngology, Juntendo University Graduate School of Medicine, Bunkyo-ku, Tokyo 113-8421 Japan

[2]Department of Biological Sciences, Louisiana State University, Baton Rouge, LA 70803

[3]Department of Cellular and Molecular Neuropathology, Juntendo University Graduate School of Medicine, Bunkyo-ku, Tokyo 113-8421 Japan

[4]Department of Physiology, Keio University School of Medicine, Shinjuku-ku, Tokyo 160-8582 Japan

Correspondence should be addressed to Junko Murata, Department of Otorhinolaryngology, Juntendo University Graduate School of Medicine, 2-1-1, Hongo, Bunkyo-ku, Tokyo 113-8421 Japan. E-mail: jmurata@juntendo.ac.jp, Phone: +81-3-5802-1229, Fax: +81-3-5840-7103

Number of pages: 37

Number of figures: 5, Number of tables: 1

Grant information: This work was supported by grants-in-Aid for Scientific Research (23592496) from JSPS (J.M.), and also supported in part by Research Institute for Diseases of Old Age, Institute for Environmental and Gender-specific Medicine of Juntendo University (J.M.).

Abstract

The present study was conducted to elucidate the presence of the melastatin-related subfamily of transient receptor potential channels, TRPM4, in the mouse inner ear. TRPM4 immunoreactivity (IR) was found in: (a) the cell body of inner hair cells (IHCs) in the Organ of Corti, (b) the apical side of marginal cells of the stria vascularis, (c) the apical portion of the dark cells of the vestibule, and (d) a subset of the type II neurons in the spiral ganglion. Subsequently, changes in the distribution and expression of TRPM4 in the inner ear during embryonic and postnatal developments were also evaluated. Immunohistochemical localization demonstrated that the emergence of the TRPM4-IR in IHCs occur shortly before the onset of hearing, while that in the marginal cells happens earlier at the time of birth coinciding with the onset of endolymph formation. Furthermore, semi-quantitative real-time PCR assay showed that expressions of TRPM4 in the Organ of Corti and in the stria vascularis increased dramatically at the onset of hearing. Because TRPM4 is a Ca^{2+}-activated monovalent selective cation channel, these findings imply that TRPM4 contributes in potassium ion transport essential for the signal transduction in IHCs and the formation of endolymph by marginal cells.

Key words

TRP channel, Endolymph, Inner hair cell, Stria vascularis, Marginal cell

Introduction

When acoustic stimuli reach the cochlea as fluid pressure waves, the basilar membrane, underlying the organ of Corti, is put into motion. This vibration elicits the deflection of stereocillia, cytoplasmic extensions of the hair cells (HCs), and causes opening of mechanoelectrical transduction channels to cations in the endolymph (Fig. 1A), a fluid compartment high in the potassium concentration. As the cochlear endolymph is high in K^+ (~150mM) and low in Na^+ (~2mM) and Ca^{2+} (~20 μM） with positive endocochlear potential (EP) of +80 mV (Von Bekesy 1952), the process allows K^+ to flow into HCs to induce their electrical excitation (Hudspeth 1989; Hudspeth and Corey 1977). Then K^+ exits across their basolateral membranes through K^+ channels and reaches the lateral wall of the cochlea (Zdebik et al. 2009) (Fig.1A).

The lateral wall of the cochlea is formed of the spiral ligament and the stria vascularis. The connective tissue of the spiral ligament contains five types of fibrocytes (Type

I-V). The stria vascularis is an epithelial tissue, and is composed of marginal, intermediate, and basal cells (Fig. 1A). The basal and intermediate cells and nearby fibrocytes are connected tightly, forming one functional layer (the basal-intermediate cell layer) (Cohen-Salmon et al. 2002; Nin et al. 2008), and the marginal cells constitute a monolayer. The extracellular space between the basal-intermediate cell and the marginal cell layers is called the intrastrial space (IS). After reaching the lateral wall of the cochlea, K^+ is transported from perilymph to the basal-intermediate cell layer of the stria vascularis, and subsequently moved in to IS (Hibino et al. 2010). K^+ is taken up from IS into the marginal cells (Kerr et al. 1982; Wangemann et al. 1995) and released finally into the endolymph through KCNQ1/KCNE1 heterometric channels in the apical membrane of marginal cells (Marcus and Shen 1994; Sakagami et al. 1991).

The cloning of the transient receptor potential (TRP) channel protein in 1989 (Montell and Rubin 1989) led to the discovery of a large family of Ca^{++}-activated non-selective cation channels that were molecularly unidentified previously. Of twenty-nine identified mammalian TRP channels, two of the melastatin-related subfamily, TRPM4 and TRPM5 (TRP melastin-related subfamily member 4 and 5), are the only monovalent selective cation channels (Guinamard et al. 2010). TRPM4 and TRPM5 are both activated by increasing intracellular Ca^{2+}

(Launay et al. 2002; Nilius et al. 2004; Zhang et al. 2007). TRPM4 is activated when internal ATP is decreased, while TRPM5 is not ATP-sensitive (Nilius et al. 2005; Ullrich et al. 2005). TRPM4 was cloned as a 1,214-amino acid molecule encoded by a gene located on human chromosome 19 (Launay et al. 2002). TRPM4 is expressed and functions in a wide variety of cell types, including inspiratory neurons (Mironov 2008), cardiomyocytes (Guinamard et al. 2004), and cerebral atrial myocytes (Earley et al. 2004). TRPM4 is also found in epithelial systems, including renal tubules (Chraibi et al. 1994; Guinamard et al. 2012).

Early investigations of the inner ear indicated the presence of TRPM4 transcripts (Cuajungco et al. 2007) and TRPM4 protein in the murine organ of the Corti. Moderate TRPM4-IR was detected in cochlear supporting cells, and the only faint TRPM4-IR was observed in stria vascularis, vestibular HCs, spiral ganglion and vestibular ganglion cells (Takumida et al. 2009). The present investigation was carried out to further characterize the expression pattern of TRPM4 during development.

Materials and Methods

Animals

C57BL/6J mice were obtained from SRL Inc. (Shizuoka, Japan) for this study. Embryonic day 0.5 (E0.5) was defined as noon of the day on which a vaginal plug was observed. The day of birth was designated as postnatal day 0 (P0). All experimental protocols were approved by the Animal Research Committee at the Juntendo University School of Medicine (the approval number: 240107, 250227), and were conducted in accordance with the U.S. National Institutes *Guide for the Care and Use of Laboratory Animals.*

Antibodies

A polyclonal anti-TRPM4 antibody was generated in rabbit by immunizing with a 15-amino acid synthetic peptide corresponding to amino acids 60–74 (NH2-TEWNSDEHTTEKPTDC-COOH) of the amino-terminal tail of the rat TRPM4 with an added carboxyl-terminal cysteine (Teruyama et al. 2011). The antiserum was affinity-purified on a column made with the synthetic peptides to produce the anti-TRPM4 rabbit polyclonal antibody (77.5 μg/ml) (Teruyama et al. 2011). This antibody recognizes a predominant band of ~134 kDa corresponding to the predicted molecular weight of TRPM4 on an immunoblot run

using a membrane fraction of MCF-7 cells (Supplementary Fig. 1). The anti-TRPM4 antibody was used at 1:1,000. The other primary antibodies used and their dilutions are as follows: rabbit polyclonal anti-Myosin VI antibody (1:300) (Proteus Biosciences, Inc., Ramona, CA, US), rat monoclonal anti-neurofilament H antibody (1:500) (EMD Millipore Co., Billerica, MA, US), mouse monoclonal anti-β-tubulin, class III antibody (TUJ1) (1:100) (EMD Millipore Co.). The characterization of these commercial primary antibodies by western blot is described in each datasheet.

Immunohistochemistry

Adult mice and pups were deeply anesthetized with pentobarbital. Embryos were removed from deeply anesthetized mothers by cesarean section, and cooled on ice. Adult mice, pups and embryos were perfused through the left ventricle using 4% paraformaldehyde (PFA) in 0.1 M phosphate buffer (pH 7.4) (PB). The temporal bones were dissected and post fixed overnight at 4°C. The temporal bones collected from mice older than seven-day-old were further decalcified in 5% EDTA in 0.1 M PB for one week. The specimens were cryoprotected in 30% sucrose in 0.1 M phosphate saline buffer (PBS) overnight at 4°C, then embedded and

frozen in Tissue-Tek OCT compound 4583 (Sakura Fine Technical Co. Ltd. Tokyo, Japan). The cochleae were sectioned at 8 μm by a cryostat and affixed to MAS-coated glass slides (Matsunami Glass, Osaka, Japan). At least three tissue sections were collected from a single cochlea. Cochleae were collected from three mice for each developmental stage of E15.5, P0, P7, 2-week-old, and 4-week-old mice. For immunohistochemistry of TRPM4, antigen retrieval was accomplished by immersing the slides in boiled 0.01 mol/L citrate buffer (pH 6.0) for 10 minutes, followed by three consecutive washes in tris buffered saline (pH 7.4) (TBS). The sections were then permeabilized in TBS containing 0.05% Tween20 (TBS-T) for 10 minutes and treated with 3% hydrogen peroxide in methanol for 10 minutes. Subsequently, the sections were blocked with TNB Blocking Buffer (PerkinElmer Inc., Waltham, MA, US) for 30 minutes at room temperature. Following overnight incubation with the anti-TRPM4 antibody (1:1000 in TNB) at 4°C, the sections were incubated in a biotinylated donkey anti-Rabbit IgG antibody (Jackson ImmunoResearch Labs Inc., West Grove, PA, US) diluted in TNB (1:200) for one hour at room temperature. The antibodies were visualized using the TSA Fluorescence System (Fluorescein) (PerkinElmer Inc.) according to the manufacturer's directions. For double immunostaining with TRPM4, either Alexa Fluor 594 conjugated donkey anti-mouse IgG

(1:400) or donkey anti-rat IgG (Life Technologies Inc., Carlsbad, PA, US) (1:400) secondary antibody was used with the biotinylated donkey anti-rabbit IgG antibody described above. The sections were counterstained with DAPI (Life Technologies Inc.), washed with TBS, and–mounted. All the confocal fluorescence images were obtained with a laser-scanning microscope (Leica TCS-SP5).

Spiral ganglion neurons (SGNs) in the mature cochlea are composed of two neuron types: Type I neurons that comprise the majority of the SGN and innervate IHCs, and smaller type II neurons that are localized laterally in the SG and innervate OHCs. Because β-III-tubulin in the cell body of type II neurons gradually declines during development while that in type I neurons remain unchanged (Barclay et al. 2011), the labeling of β-III-tubulin and TRPM4 were used together to identify whether type I or Type II SGN express TRPM4.

The results of immunohistochemistry were summarized in Table 1. The intensity of TRPM4-immunoreactivity (IR) was described as follows. (+++): Intensive IR was detected. (++): IR was definitely detected, but it was not so intensive. (+): Only diffuse IR was detected. (-): IR was not detected at all.

Western blot analysis of TRPM4

Cell culture: MCF-7 cells (Soule et al. 1973) were cultured at 37C in 5% CO_2 in Dulbecco's Modified Eagle's medium, High Glucose (Life Technologies), supplemented with 10% (v/v) Fetal Bovine serum (Life Technologies).

Extraction of membrane protein: The membrane fraction was prepared from cultured MCF-7 cells as follows (Tesfai et al. 2001): A pellet of MCF-7 cells (2 x 10^7 cells) was suspended in ice-cold extraction buffer (50mM Tris/HCl, 1mM EDTA, 1% (v/v) ProteoGuard EDTA-Free Protease Inhibitor Cocktail (pH 7.5; Clontech Laboratories, Inc., Mountain View, CA, US)), and homogenized using a glass-glass homogenizer. Homogenates were centrifuged at 8,000 g for 10min at 4°C to remove cellular debris. The supernatant was centrifuged at 50,000 g for 30 min at 4°C to precipitate the membrane fraction. The pellet was re-suspended in chilled extraction buffer containing 1% (v/v) Triton X-100.

Western blot analysis: 10μg of MCF-7 whole cell lysate (Abcam plc., Cambridge Science Park, Cambridge, UK) and 5μg of MCF-7 membrane fraction were respectively solubilized in equal volumes of Laemmli Sample Buffer containing 5% 2-mercaptoethanol, and incubated at 37°C for an hour (Drew et al. 2006). SDS/PAGE was performed on Mini-PROTEAN TGX Precast Gels 4-20% (Bio-Rad Laboratories, Inc., Berkeley, CA, US) and

transferred electrophoretically to PVDF membrane (Trans-Blot Turbo Transfer Pack, PVDF, 7x 8.5 cm; Bio-Rad). The membrane was blocked for 30min at room temperature in TBS-T (Tris buffered saline: containing 20mM Tris/HCl, 500mM NaCl, 0.1% (v/v) Tween 20; pH 8.0) with 5% (w/v) skimmed-milk powder, and incubated with anti-TRPM4 antibody ($155x10^{-3}$µg/ml in TBS-T) overnight at 4°C. After washing, the membrane was incubated with peroxidase conjugated secondary antibody (1:5,000 in TBS-T) (GE, Fairfield, CT, UA) for 3h at room temperature. The sites of antibody-antigen reaction were visualized with enhanced chemiluminescence (SuperSignal West Dura Extended Duration Substrate; ThermoFisher Scientific, Inc., Waltham, MA, US) and scanned by C-DiGit (LI-COR, Inc., Lincoln, NE, USA).

Semi-quantitative real-time reverse transcriptase-polymerase chain reaction (qRT-PCR)

Cochleae were dissected from six mice for each developmental stage of E15.5, E17.5, P0, P2, P7, 2-week-old, and 4-week-old. The Organ of Corti and the lateral wall were carefully dissected from spiral ganglion neurons and other surrounding tissue and saved separately in RNAlater (Life Technologies). After homogenization in RLP-βME buffer (QIAGEN, Venlo, Netherland), total RNA was isolated using RNeasy Micro Kit (Qiagen) and quantified by the NanoDrop 1000 spectrophotometer (ThermoFisher Scientific Inc.). The total RNA (0.2-0.8

μg) was annealed to random primer and reverse transcribed to cDNA using the PrimeScript II 1st strand cDNA Synthesis Kit (TAKARA BIO Inc., Shiga, Japan). Semi-quantitative RT-PCR (qRT-PCR) for *TRPM4* was performed with the TaqMan Fast Advanced Master Mix using the Applied Biosystems 7500 FAST system (Life Technologies Inc.). The expression of *TRPM4* was normalized by the expression of ribosomal protein, large, P0 (*Rplp0*), to compensate the variation in the quality of RNA and the amount of cDNA. The RT-PCR reaction for each sample was performed in triplicate. To analyze the RT-PCR results, the average cycle threshold value (Ct) was determined for each reaction. Differences in Ct (ΔCt) between *Rplp0* and *TRPM4* were calculated by subtracting the Ct of *TRPM4* from Ct of *Rplp0*. Changes in the expression of TRPM4 during the development relative to its expression in E15.5 were obtained by subtracting mean ΔCt from each developmental stage from that of E15.5 and expressed as $2^{\Delta Ct}$. TaqMan® Gene Expression Assays (Life Technologies Inc.) used were *Rplp0* (Mm00725448_s1), and *TRPM4* (Mm00613173_m1).

Results

TRPM4-immunoreactivity was observed in the cochlea

Immunofluorescence microscopy demonstrated several TRPM4-immunoreactive structures in the cochlea from two-week-old mice. A robust TRPM4-Immunorectivity (IR) was observed in the apical layer of the stria vascularis, in IHCs of the organ of Corti, and in a subset of the spiral ganglion cells and the nerve fibers (Fig. 2A). To confirm the specificity of the anti-TRPM4 antibody, we performed an antibody absorption test; the cochlear sections from four-week-old mice were incubated with the anti-TRPM4 antibody (0.075μg/ml) that were pre-incubated with its antigen (60-74) (0.1μg/ml). No immunoreactivity was observed in preabsorbed controls (Fig. 2B) while staining without pre-absorption had the similar TRPM4-IR distribution to that from two-week-old mice (Fig 2C).

TRPM4 was distinctly localized in soma of inner hair cells and in the apical side of the marginal cells

In the organ of Corti of four-week-old mice, a robust TRPM4-IR was localized in IHCs (Fig. 3A). A weak and diffuse TRPM4-IR was also found in OHCs, inner pillar cells (IPs) and outer pillar cells (OPs), and Deiters' cells (DCs) (Fig. 3A). To clarify the location of TRPM4 within the IHC, a section nearby to that used in Fig. 3A was immunolabeled with the rabbit

anti-Myosin VI antibody (Fig. 3B). Myosin VI is located throughout the cell body of HCs but is conspicuously concentrated in the pericuticular necklace and basolateral region (Roux et al. 2009). TRPM4-IR was localized throughout the cell body of IHCs (Fig. 3A and 3B). Double immunofluorescence was also performed to localize of TRPM4 and neurofilament H (NFH) in the organ of Corti (Fig. 3C-E). TRPM4-IR of IHC was not attributable to nerve fibers that were immunolabeled with the anti-NFH antibody, although a subset of the fibers were immunoreactive for TRPM4 (white arrowheads in Fig. 3C-E). Labeling of cell nuclei with DAPI clearly demonstrated the location of basal cells, intermediate cells, and marginal cells in the stria vascularis (Fig. 3F). TRPM4-IR was concentrated toward the apical membrane of marginal cells.

The details of the distribution of TRPM4 in the spiral ganglion (SG) were further examined in the cochlea of a four-week-old mouse. Intense TRPM4-IR was observed in smaller spiral ganglion neurons (SGNs) in the lateral portion of the SG (yellow arrowheads in Fig. 3G). Less intense TRPM4-IR was also observed in the larger cell bodies of SGNs located in the rest of the SG (white arrowheads in Fig. 3G, I). The smaller cells that had intense TRPM4-IR (yellow arrowheads in Fig. 3G, I) were nearly immnonegative to β-III-tubulin (Fig. 3H, I),

putative type II SGNs. In contrast, the larger cells that were strongly immunoreactive to β-III-tubulin, putative Type I SGNs (white arrowheads in Fig. 3H, I), were only weakly immunoreactive to TRPM4 (Fig. 3G, I).

TRPM4-immuoreactivity is concentrated toward the apical membrane of dark cells in the vestibular labyrinth.

Immunohistochemical localization of TRPM4 was also examined in the lateral semicircular canal of the vestibule from two-week-old mice. Each semicircular canal contains a sensory epithelium, the crista ampullaris, which is a thickened epithelial ridge oriented perpendicular to the long axis of the duct. The crista ampullaris is surrounded by a non-sensory transitional epithelium (TE; Fig. 4A), which continues to the dark cells regions. Intense TRPM4-IR was found in HCs of the crista ampullaris and dark cells in the lateral semicircular canal. However, no prominent TRPM4-IR was observed in the transitional cells (Fig. 4A, see also supplementary Fig. 2A, B). Furthermore, a higher power image demonstrated that TRPM4-IR is concentrated on the apical side within dark cells, although some weak immunoreactivity was also dispersed in the rest of the cell body (Fig. 4B). A section containing

the crista ampullaris of the posterior semicircular canal was double-labeled with the TRPM4 (Figure 4C: green) and NFH (Figure 4D: red). The double labeling revealed that TRPM4-IR is also localized in a subset of the vestibular nerves fibers (white arrows in Fig. 4C-E). The HCs of the crista ampullaris in a nearby section to Figures 4C-E was labeled for myosin VI immunolabeling to clarify the HC region in epithelial layer of the crista ampullaris (Fig. 4F). We observed TRPM4-IR in both types of vestibular HCs, Type I and Type II (Supplementary Fig. 3). In the vestibular ganglion located in the inner auditory meatus, weak and diffuse TRPM4-IR was barely detected in the somas of neurons (Supplementary Fig. 4).

The expression of TRPM4 in the cochlea is markedly up regulated at the onset of hearing

To investigate changes in the distribution of TRPM4 in the cochlear duct during development, TRPM4 immunohistochemistry was performed in samples obtained from E15.5, P0, P7, 2-week-, 4-week-, 8-week-, and 20-week-old mice. At E15.5, no detectable TRPM4-IR was found either in the cochlear duct (Fig. 5A) or the SG (Fig. 5B). At P0, prominent TRPM4-IR was already observed in the marginal cell layer of the stria vascularis (Fig. 5C). Faint TRPM4-IR was also observed in some somas in the SG at P0 (Fig. 5D). At P7, TRPM4-IR

in the Organ of Corti was exclusively localized at this stage in the IHCs (Fig. 5E). Moreover, weak TRPM4-IR started appearing in the neural fibers and somas of SGNs, and an additional TRPM4-IR was found in the Reissner's membrane at P7 (Fig. 5E). At two weeks of age, which corresponds to the onset of hearing (Shnerson and Pujol 1981; Wangemann 2011), intense TRPM4-IRs were present in the strial marginal cells, IHCs, the Reissner's membrane and SGNs (Fig. 5G, H). At four weeks of age, the distribution of TRPM4-IR in the cochlea remained the same as that found in two-week-old specimens (Fig. 5I). However, much of the intense immunoreactivity observed in the nerve fibers in SG from two-week-olds was diminished, and only weak TRPM4-IR was observed (Fig. 5J). There were no detectable differences in the distribution of TRPM4-IR in the cochleae from eight-week- and twenty-week-old mice compare to that from four-week-old mice (data not shown). Changes in the distribution of TRPM4-IR are summarized in Table 1.

To clarify the changes in TRPM4 expression in the cochlea during development, two tissue samples, the organ of Corti and the lateral wall containing the stria vascularis, fibrocytes, and connective tissue, were dissected from the cochlea from E17.5, P0, P2, P7, two week-, and four week- old mice. The RNA extracted from the whole cochlea was used with the sample

from E15.5 old mice. Semi-quantitative RT-PCR was performed and relative changes in TRPM4 transcripts were determined. In both the Organ of Corti and the lateral wall, there was no obvious change in the relative level of mRNA for TRPM4 until two-week-old. However, the expression surged from P7 to two-week-old when the onset of hearing occurs (Fig. 5K, L).

Discussion

The present study demonstrates that robust TRPM4-IR is specifically localized in soma of IHCs in the Organ of Corti. This suggests that TRPM4 plays a specific role related to the function of IHCs. When sound stimuli open the mechanosensory transduction channels on the stereocillia, K^+ enters and depolarizes IHCs. The depolarization opens voltage-gated Ca^{2+} channels, and the resultant Ca^{2+} influx causes transmitter release from the basal end of the cell to the auditory nerve endings. Increased intracellular Ca^{2+} could also open TRPM4 in the soma of IHCs leading to K^+ efflux and IHC repolarization. In contrast to IHCs, only diffuse and weak TRPM4-IR was observed in OHCs. The voltage-gated K^+ channel, KCNQ4, is abundantly present in OHCs at their basal membrane and is thought to mediate a major pathway for K^+ efflux (Kharkovets et al. 2006). In the cochlea of KCNQ4 knockout (KO) mice, OHCs

gradually degenerated as hearing threshold declined by ~50dB over several weeks. Interestingly, the expression of KCNQ4 is far more limited in IHCs, and IHCs are apparently unaffected in KCNQ4 KO mice (Kharkovets et al. 2006). These results suggest the presence of an additional system in IHCs that mediates repolarization through K^+ efflux. Moreover, a greater expression of TRPM4 in IHCs may be needed to compensate for the relative absence of KCNQ4. At the same time, the lower expression of TRPM4 in OHCs indicates that TRPM4 is not a major player in the repolarization of OHCs because of the abundant presence of KCNQ4. A role for TRPM4 in repolarization of the IHCs is further suggested by TRPM4-IR in the cell body without IR on the apical membrane.

Another intriguing finding in this study was the presence of TRPM4 in the apical side of the strial marginal cells. The marginal cells transport K^+ from the intrastrial space into the endolymph (Kerr et al. 1982; Wangemann et al. 1995). The K^+ efflux into the endolymph is largely conducted by voltage-dependent K^+ ion channels, KCNQ1/KCNE1 heterometric channels, which are expressed in the apical membrane of marginal cells (Marcus and Shen 1994; Sakagami et al. 1991). Indeed, the targeted disruptions of the KCNQ1/KCNE1 gene in mice lead to deafness and show gross morphological anomalies due to a drastic reduction in the

volume of endolymph (Casimiro et al. 2001; Vetter et al. 1996). While these voltage-dependent K^+ ion channels are essential for K^+ transport, the presence of non-selective cation channel was also detected by patch clamp electrophysiology in the apical membrane of marginal cells (Sunose et al. 1993; Takeuchi et al. 1992). The studies demonstrated that these cation channel are activated when intracellular concentration of Ca^{2+} reaches 10^{-5} M; this channel has a conductance of ~27 pS for monovalent cations and does not allow Ca^{2+}permeation. The physiological characteristic described above correspond to those of TRPM4 and TRPM5 channels (Guinamard et al. 2010). More importantly, the cation channel was inactivated by cytoplasmic ATP (Sunose et al. 1993). Because TRPM4 is activated when internal ATP is decreased while TRPM5 is not ATP-sensitive (Nilius et al. 2005; Ullrich et al. 2005), these findings together with our findings suggest that the marginal cells possess functional TRPM4 channels. Although the exact role for TRPM4 in the apical surface of the marginal cells is currently unknown, we speculate that TRPM4 cooperates with KCNQ1/KCNE1 channels in K^+ transport into the endolymph.

Within the spiral ganglion (SG), TRPM4-IR was almost exclusively found in small β-III-tubulin-immunonegative type II neurons. In the inspiratory neurons, TRPM4 is known to

contribute to an excitatory post-synaptic potential, which activates voltage-dependent sodium channels to induce bursting activity of the neurons (Crowder et al. 2007; Mironov 2008). Therefore, it is possible that TRPM4 in the small type II SG neurons might mediate the excitatory post-synaptic potentials necessary for these neurons. Electrophysiological experiments will be required to investigate this possibility.

The vestibular labyrinth that contains the sacculus, utriculus, and three semicircular canals, is also filled with endolymph. When the sensory epithelium in semicircular canals are stimulated by head rotations, K^+ in the vestibular endolymph (~150 mM) (Wangemann 2002) flows into HCs via the mechanotransduction channel and exits through KCNQ4 and other K^+ channels in the basolateral membrane (Kharkovets et al. 2000; Valli et al. 1990). Intense TRPM4-IR was found in HCs of the crista ampullaris and dark cells in the lateral semicircular canal. Like marginal cells in the stria vascularis, dark cells constitute a monolayer lining of the endolymphatic space and are responsible for the production of endolymph in the semicircular canal (Nakai and Hilding 1968). Dark cells are known to absorb the released K^+ (Kikuchi et al. 1994) and transport K^+ back into the endolymph via KCNQ1/KCNE1 in their apical membrane (Marcus et al. 1997; Wangemann et al. 1996). Further, non-selective cation current was

electrophysiologically detected in the apical membrane of the vestibular dark cells (Marcus et al. 1992). This finding supports our data of the unique presence of TRPM4 in the apical side of dark cells in the semicircular canal. Although an exact physiological role of TRPM4 in the vestibular dark cells is unknown, we speculate that TRPM4 contributes to maintain the high K^+ concentration of endolymph in the vestibule.

The present study also demonstrated changes in the distribution and expression of TRPM4 in the mouse cochlea during development. The formation of the endolymph starts shortly before birth when the concentration of K^+ increases while Na^+ decreases. By P0, the concentrations of K^+ and Na^+ are approximately equal (~80mM) which coincides with the onset of KCNQ1 expression in the stria vascularis (Li et al. 2013). Because TRPM4-IR was not detectable at E15.5 but clearly observed at P0, the onset of TRPM4 expression in the stria vascularis also coincides with the onset of KCNQ1 expression and endolymph formation. In addition, qRT-PCR analysis showed that TRPM4 expression was distinctly up regulated from P7 to two-week-old in the lateral wall of the cochlea and in the organ of Corti, which coincides with the onset of hearing (P12) in mice (Shnerson and Pujol 1981; Wangemann 2011). These findings are consistent with our hypothesis that TRPM4 is involved in formation of endolymph.

Another interesting finding is that while the onset of TRPM4 expression in the stria vascularis is in accord with the onset of endolymph formation, TRPM4 expression in IHCs occurs shortly before the onset of hearing. An up-regulation of TRPM4 at two-week-old would be in accord with the timeline for development of sound perception (from P6 to P15) (Wangemann 2011) and the need for mechanism to repolarize the IHC.

In summary, we demonstrated that TRPM4 channels are located on the apical side of strial marginal cells and in the basolateral portion of IHCs in the cochlea of adult mice. We also examined changes in the distribution and expression of TRPM4 during cochlear growth. The onset of TRPM4 expression in the stria vascularis coincides with the onset of endolymph formation. In contrast, the onset of TRPM4 expression in IHCs coincides with the onset of hearing. From these results, we speculate that the physiological roles of TRPM4 are related to the function of strial marginal cells and IHCs, the formation of endolymph and the sensory cell repolarization, respectively.

Acknowledgement

We are grateful to Prof. Makoto Tominaga (National Institute for Physiological

Sciences), Dr. Makoto Hosoya (Keio University) and Dr. Masato Fujioka (Keio University) for their critical reading of the manuscript. We profoundly thank Drs. Tomomi Ikeda and Takako Ikegami (Juntendo University) for their technical advice in real-time PCR quantification, Dr. Shinji Nakamura (Juntendo University) for his technical assistance in immunohistochemistry using the enzyme labeled antibody method, and Dr. Tsutomu Fujimura (Juntendo University) for the synthesis of the antigen peptide and his technical advice in western blotting. The authors declare we have no conflict of interest.

References

Barclay M, Ryan AF, Housley GD. 2011. Type I vs type II spiral ganglion neurons exhibit differential survival and neuritogenesis during cochlear development. Neural development 6:33.

Casimiro MC, Knollmann BC, Ebert SN, Vary JC, Jr., Greene AE, Franz MR, Grinberg A, Huang SP, Pfeifer K. 2001. Targeted disruption of the Kcnq1 gene produces a mouse model of Jervell and Lange-Nielsen Syndrome. Proceedings of the National Academy of Sciences of the United States of America 98(5):2526-2531.

Chraibi A, Van den Abbeele T, Guinamard R, Teulon J. 1994. A ubiquitous non-selective cation channel in the mouse renal tubule with variable sensitivity to calcium. Pflugers Archiv : European journal of physiology 429(1):90-97.

Cohen-Salmon M, Ott T, Michel V, Hardelin JP, Perfettini I, Eybalin M, Wu T,

Marcus DC, Wangemann P, Willecke K, Petit C. 2002. Targeted ablation of connexin26 in the inner ear epithelial gap junction network causes hearing impairment and cell death. Current biology : CB 12(13):1106-1111.

Crowder EA, Saha MS, Pace RW, Zhang H, Prestwich GD, Del Negro CA. 2007. Phosphatidylinositol 4,5-bisphosphate regulates inspiratory burst activity in the neonatal mouse preBotzinger complex. The Journal of physiology 582(Pt 3):1047-1058.

Cuajungco MP, Grimm C, Heller S. 2007. TRP channels as candidates for hearing and balance abnormalities in vertebrates. Biochimica et biophysica acta 1772(8):1022-1027.

Drew D, Lerch M, Kunji E, Slotboom DJ, de Gier JW. 2006. Optimization of membrane protein overexpression and purification using GFP fusions. Nature methods 3(4):303-313.

Earley S, Waldron BJ, Brayden JE. 2004. Critical role for transient receptor potential channel TRPM4 in myogenic constriction of cerebral arteries. Circulation research 95(9):922-929.

Guinamard R, Chatelier A, Demion M, Potreau D, Patri S, Rahmati M, Bois P. 2004. Functional characterization of a Ca(2+)-activated non-selective cation channel in human atrial cardiomyocytes. The Journal of physiology 558(Pt 1):75-83.

Guinamard R, Demion M, Launay P. 2010. Physiological roles of the TRPM4 channel extracted from background currents. Physiology (Bethesda, Md) 25(3):155-164.

Guinamard R, Paulais M, Lourdel S, Teulon J. 2012. A calcium-permeable non-selective cation channel in the thick ascending limb apical membrane of the mouse kidney. Biochimica et biophysica acta 1818(5):1135-1141.

Hibino H, Nin F, Tsuzuki C, Kurachi Y. 2010. How is the highly positive endocochlear potential formed? The specific architecture of the stria vascularis and the roles of the ion-transport apparatus. Pflugers Archiv : European journal of physiology 459(4):521-533.

Hudspeth AJ. 1989. How the ear's works work. Nature 341(6241):397-404.

Hudspeth AJ, Corey DP. 1977. Sensitivity, polarity, and conductance change in the response of vertebrate hair cells to controlled mechanical stimuli. Proceedings of the National Academy of Sciences of the United States of America 74(6):2407-2411.

Kerr TP, Ross MD, Ernst SA. 1982. Cellular localization of Na+,K+-ATPase in the mammalian cochlear duct: significance for cochlear fluid balance. American journal of otolaryngology 3(5):332-338.

Kharkovets T, Dedek K, Maier H, Schweizer M, Khimich D, Nouvian R, Vardanyan V, Leuwer R, Moser T, Jentsch TJ. 2006. Mice with altered KCNQ4 K+ channels implicate sensory outer hair cells in human progressive deafness. The EMBO journal 25(3):642-652.

Kharkovets T, Hardelin JP, Safieddine S, Schweizer M, El-Amraoui A, Petit C, Jentsch TJ. 2000. KCNQ4, a K+ channel mutated in a form of dominant deafness, is expressed in the inner ear and the central auditory pathway. Proceedings of the National Academy of Sciences of the United States of America 97(8):4333-4338.

Kikuchi T, Adams JC, Paul DL, Kimura RS. 1994. Gap junction systems in the rat vestibular labyrinth: immunohistochemical and ultrastructural analysis. Acta oto-laryngologica 114(5):520-528.

Launay P, Fleig A, Perraud AL, Scharenberg AM, Penner R, Kinet JP. 2002. TRPM4 is a Ca2+-activated nonselective cation channel mediating cell membrane depolarization. Cell 109(3):397-407.

Li X, Zhou F, Marcus DC, Wangemann P. 2013. Endolymphatic Na(+) and K(+) Concentrations during Cochlear Growth and Enlargement in Mice Lacking Slc26a4/pendrin. PloS one 8(5):e65977.

Marcus DC, Shen Z. 1994. Slowly activating voltage-dependent K+ conductance is apical pathway for K+ secretion in vestibular dark cells. The American journal of physiology 267(3 Pt 1):C857-864.

Marcus DC, Sunose H, Liu J, Shen Z, Scofield MA. 1997. P2U purinergic receptor inhibits apical IsK/KvLQT1 channel via protein kinase C in vestibular dark cells. The American journal of physiology 273(6 Pt 1):C2022-2029.

Marcus DC, Takeuchi S, Wangemann P. 1992. Ca(2+)-activated nonselective

cation channel in apical membrane of vestibular dark cells. The American journal of physiology 262(6 Pt 1):C1423-1429.

Mironov SL. 2008. Metabotropic glutamate receptors activate dendritic calcium waves and TRPM channels which drive rhythmic respiratory patterns in mice. The Journal of physiology 586(9):2277-2291.

Montell C, Rubin GM. 1989. Molecular characterization of the Drosophila trp locus: a putative integral membrane protein required for phototransduction. Neuron 2(4):1313-1323.

Nakai Y, Hilding D. 1968. Vestibular endolymph-producing epithelium. Electron microscopic study of the development and histochemistry of the dark cells of the crista ampullaris. Acta oto-laryngologica 66(1):120-128.

Nilius B, Prenen J, Janssens A, Voets T, Droogmans G. 2004. Decavanadate modulates gating of TRPM4 cation channels. The Journal of physiology 560(Pt 3):753-765.

Nilius B, Prenen J, Tang J, Wang C, Owsianik G, Janssens A, Voets T, Zhu MX. 2005. Regulation of the Ca2+ sensitivity of the nonselective cation channel TRPM4. The Journal of biological chemistry 280(8):6423-6433.

Nin F, Hibino H, Doi K, Suzuki T, Hisa Y, Kurachi Y. 2008. The endocochlear potential depends on two K+ diffusion potentials and an electrical barrier in the stria vascularis of the inner ear. Proceedings of the National Academy of Sciences of the United States of America 105(5):1751-1756.

Roux I, Hosie S, Johnson SL, Bahloul A, Cayet N, Nouaille S, Kros CJ, Petit C, Safieddine S. 2009. Myosin VI is required for the proper maturation and function of inner hair cell ribbon synapses. Human molecular genetics 18(23):4615-4628.

Sakagami M, Fukazawa K, Matsunaga T, Fujita H, Mori N, Takumi T, Ohkubo H, Nakanishi S. 1991. Cellular localization of rat Isk protein in the stria vascularis by immunohistochemical observation. Hearing research 56(1-2):168-172.

Shnerson A, Pujol R. 1981. Age-related changes in the C57BL/6J mouse

cochlea. I. Physiological findings. Brain research 254(1):65-75.

Soule HD, Vazguez J, Long A, Albert S, Brennan M. 1973. A human cell line from a pleural effusion derived from a breast carcinoma. Journal of the National Cancer Institute 51(5):1409-1416.

Sunose H, Ikeda K, Saito Y, Nishiyama A, Takasaka T. 1993. Nonselective cation and Cl channels in luminal membrane of the marginal cell. The American journal of physiology 265(1 Pt 1):C72-78.

Takeuchi S, Marcus DC, Wangemann P. 1992. Ca(2+)-activated nonselective cation, maxi K+ and Cl- channels in apical membrane of marginal cells of stria vascularis. Hearing research 61(1-2):86-96.

Takumida M, Ishibashi T, Hamamoto T, Hirakawa K, Anniko M. 2009. Expression of transient receptor potential channel melastin (TRPM) 1-8 and TRPA1 (ankyrin) in mouse inner ear. Acta oto-laryngologica 129(10):1050-1060.

Teruyama R, Sakuraba M, Kurotaki H, Armstrong WE. 2011. Transient receptor potential channel m4 and m5 in magnocellular cells in rat supraoptic and paraventricular nuclei. Journal of neuroendocrinology 23(12):1204-1213.

Tesfai Y, Brereton HM, Barritt GJ. 2001. A diacylglycerol-activated Ca2+ channel in PC12 cells (an adrenal chromaffin cell line) correlates with expression of the TRP-6 (transient receptor potential) protein. The Biochemical journal 358(Pt 3):717-726.

Ullrich ND, Voets T, Prenen J, Vennekens R, Talavera K, Droogmans G, Nilius B. 2005. Comparison of functional properties of the Ca2+-activated cation channels TRPM4 and TRPM5 from mice. Cell calcium 37(3):267-278.

Valli P, Zucca G, Botta L. 1990. Perilymphatic potassium changes and potassium homeostasis in isolated semicircular canals of the frog. The Journal of physiology 430:585-594.

Vetter DE, Mann JR, Wangemann P, Liu J, McLaughlin KJ, Lesage F, Marcus DC, Lazdunski M, Heinemann SF, Barhanin J. 1996. Inner ear defects induced by null mutation of the isk gene. Neuron 17(6):1251-1264.

Von Bekesy G. 1952. Resting potentials inside the cochlear partition of the guinea pig. Nature 169(4293):241-242.

Wangemann P. 2002. K(+) cycling and its regulation in the cochlea and the vestibular labyrinth. Audiology & neuro-otology 7(4):199-205.

Wangemann P. 2011. The role of pendrin in the development of the murine inner ear. Cellular physiology and biochemistry : international journal of experimental cellular physiology, biochemistry, and pharmacology 28(3):527-534.

Wangemann P, Liu J, Marcus DC. 1995. Ion transport mechanisms responsible for K+ secretion and the transepithelial voltage across marginal cells of stria vascularis in vitro. Hearing research 84(1-2):19-29.

Wangemann P, Shen Z, Liu J. 1996. K(+)-induced stimulation of K+ secretion involves activation of the IsK channel in vestibular dark cells. Hearing research 100(1-2):201-210.

Zdebik AA, Wangemann P, Jentsch TJ. 2009. Potassium ion movement in the inner ear: insights from genetic disease and mouse models. Physiology (Bethesda, Md) 24:307-316.

Zhang Z, Zhao Z, Margolskee R, Liman E. 2007. The transduction channel TRPM5 is gated by intracellular calcium in taste cells. The Journal of neuroscience : the official journal of the Society for Neuroscience 27(21):5777-5786.

Figure legends

Fig. 1 Schematic drawing of the cochlear duct of mice

A: A cross-section of the cochlear duct was schematically drawn to indicate the flow of K^+. The scala media is filled with endolymph, an unusual extracellular fluid (high in K^+ and low in Na^+ and Ca^{2+}) resulting in a positive endocochlear potential of +80 mV. The lateral cochlear wall is formed of two components: (1) spiral ligaments, the connective tissue containing five types of fibrocytes (Type I –V; indicated as I –V), and (2) the stria vascularis (SV) which is epithelial tissue composed of marginal (M), intermediate (I), and basal (B) cells. The organ of Corti (OC) represents the sensory epithelium of the cochlea and contains sensory IHCs and OHCs with associated supporting cells. Sound induced mechanical vibration moves the basilar membrane of the OC. The afferent and efferent neurons from the spiral ganglion (SG) innervate the IHCs and OHCs.

Fig. 2 Immunohistochemical localization of the TRPM4 channel in the mouse cochlea

A: Robust immunoreactivity (IR) of TRPM4 was observed in marginal cells of the stria vascularis, IHCs of the Organ of Corti, and a part of the spiral ganglion cells and their processes

from a two-week-old mouse. **B**: The result of an antibody absorption test: A cochlear section pre-absorbed with the antigen peptide (0.1μg/ml) showed no IR. **C**: TRPM4-IR in the control section of a four-week-old mouse without pre-absorption: TRPM4-IR was observed in the marginal cell layer of the stria vascularis, IHCs of the Organ of Corti and a part of the spiral ganglion cells and their processes. The distribution of TRPM4-IR from the cochlea of a four-week -old mouse was essentially identical to that seen in A. Scale bar: 100 μm in **A-C**.

Fig. 3 Localization of the TRPM4 channel in the soma of IHCs and in the apical membrane of the strial marginal cells

A: A robust TRPM4-IR (green) was localized to IHCs, whereas diffuse IR was found in OHCs, the inner pillar (IP), the outer pillar (OP), and in Deiters' (DC) cells in the Organ of Corti from the cochlear turn of a four-week-old mouse. Nuclei were counterstained by DAPI (blue). **B**: A section adjacent to that used in A was immunostained for Myosin VI antibody (red). Myosin VI is located the hair cells except in the hair bundle; however, myosin VI is particularly concentrated in the cuticular plate and the pericuticular necklace region. Note that TRPM4-IR was not observed in the subcellular region where a high concentration of Myosin VI-IR would

be observed in A. This indicates that TRPM4- IR was solely in the soma under the circumferential band, which has access to the perilymph but not to the endolymph. **C**: An adjacent section to B was immunostained for TRPM4 (green). **D**: The same section used in C was also immunostained for neurofilament H (red: NFH). **E**: A merged image of C and D showed that TRPM4-IR of IHCs did not originate from the innervating axons, although a subset of the axons did express TRPM4 (a white arrow head). **F**: A section including the stria vascularis from a four-week-old mouse was immunostained for TRPM4 (green). The counter staining of the cell nuclei with DAPI (blue) allows for the nuclei of basal cells, intermediate cells, and marginal cells to be distinguished. The results clearly show that TRPM4-IR is localized in the apical surface of the marginal cells. Scale bar: 30 μm in A-F. **G&H**: A section of the spiral ganglion from a four-week-old mouse was immunostained for TRPM4 (green: **G**) and β-III-tubulin (red: **H**). **I**: A merged image of G and H. A robust TRPM4-IR was observed in small, β-III-tubulin-immuonegative type II neurons (yellow arrowheads) that innervate OHCs. In contrast, only faint TRPM4-IR was observed in large β-III-tubulin-immunopositive type I neurons that innervate IHCs. Note the relatively reddish cell body with small yellow granules (white arrowheads). Scale bars: 50 μm in **G**-**H**.

Fig. 4 TRPM4-IR was observed in hair cells and in the apical side of dark cells, but not in the transitional cells of the vestibular epithelium

A: The vestibular labyrinth contains a sacculus, a utriculus, and three semicircular canals filled with endolymph. The crista ampullaris (CA) is the sensory epithelium of the semicircular canals. The transitional epithelium (TE) that surrounds the crista ampullaris continues to the non-sensory epithelial cells, the dark cells (DC). Like strial marginal cells, vestibular dark cells also take up K^+ from their basolateral membranes and release it into the endolymph at their apical membrane. A section from the lateral semicircular canal of a two-week-old mouse was immunostained for TRPM4 (green) with DAPI counterstaining for the cell nuclei (blue). TRPM4-IR was observed in the sensory epithelium (crista ampullaris) and dark cell region; however, no TRPM4-IR was found in the transitional epithelium. Scale bar: 50 μm. **B**: The dark cell layer in A is enlarged. TRPM4-IR was concentrated in the luminal (apical) side of the dark cells (white arrow heads). Scale bar: 20μm. **C&D**: A section from the posterior semicircular canal of a 4-week-old mouse was immunostained for TRPM4 (green) (**C**) and neurofilament H (NFH) (red) (**D**). **E**: Merged image of **C** and **D**. A mammalian vestibular organ contains two

types of hair cells, type I and type II. The basolateral surface of type I hair cell is enveloped by a single large afferent nerve terminal, which is called calyx (white arrowheads in **C-E**). TRPM4-IR was not observed in the calyces (white arrowheads in **C-E**). On the other hand, TRPM4-IR was observed in the more central region of some vestibular nerve fibers (white arrows in **C-E**). **F**: A nearby section was immunostained for myosin VI (red). Note that the cells that possess TRPM4-IR in **C** were myosin VI- immunopositive HCs (yellow arrows in **C & F**). Scale bars: 50 μm in **C-F**

Fig. 5 The expression of TRPM4 in the cochlea is markedly up-regulated at the onset of hearing

Changes in the distribution of TRPM4-IR were examined in the cochlear duct (**A, C, E, G, I**) and spiral ganglion (SG) (**B, D, F, H, J**) during development. The nuclei were counterstained by DAPI (blue). **A&B**: At E15.5, no TRPM4-IR was found in the cochlear duct or in the SG. **C**: At P0, a moderate TRPM4-IR was already observed in the stria vascularis (SV). **D**: At P0, a weak TRPM4-IR was observed in some spiral ganglion neurons. **E**: At P7, a noticeable TRPM4-IR was localized to IHCs of the Organ of Corti. The IR in marginal cells of the SV became

prominent at this stage. IR was also localized to the Reissner's membrane (RM). **F**: There was no noticeable difference in TRPM4-IR in the SG between P0 and P7, whereas some spiral ganglion neurons were still immunoreactive to TRPM4. **G**: Intense TRPM4-IRs in 2-week-old mice were observed in the strial marginal cells and IHCs (white arrow), corresponding to the onset of hearing. **H**: In addition to the spiral ganglion neurons, TRPM4-IR was also observed at 2 weeks of age in the nerve fibers in the SG. **I**: At four weeks, the distribution of TRPM4-IR in the cochlea remained the same as that found at two weeks of age. **J**: Intense TRPM4-IR in the nerve fibers observed in SG from two-week-old mice was diminished at 4-week-old (white arrowheads). Scale bar: 50 μm in **A**-**J**. To evaluate changes in TRPM4 transcript expression in the Organ of Corti and stria vascularis during development, semi-quantitative RT-PCR was performed on mRNA extracted from the Organ of Corti and from the lateral wall that contains the stria vascularis from mice ages between E15.5 and four-week-old. **K**: In the organ of Corti, the relative level of m RNA for TRPM4 surged up from P7 to two-week-old concurrent with the onset of hearing. **L**: The relative level of mRNA for TRPM4 in the lateral wall was also markedly increased from P7 to two weeks of age. The error bar indicates a standard deviation of the mean in **K&L**.

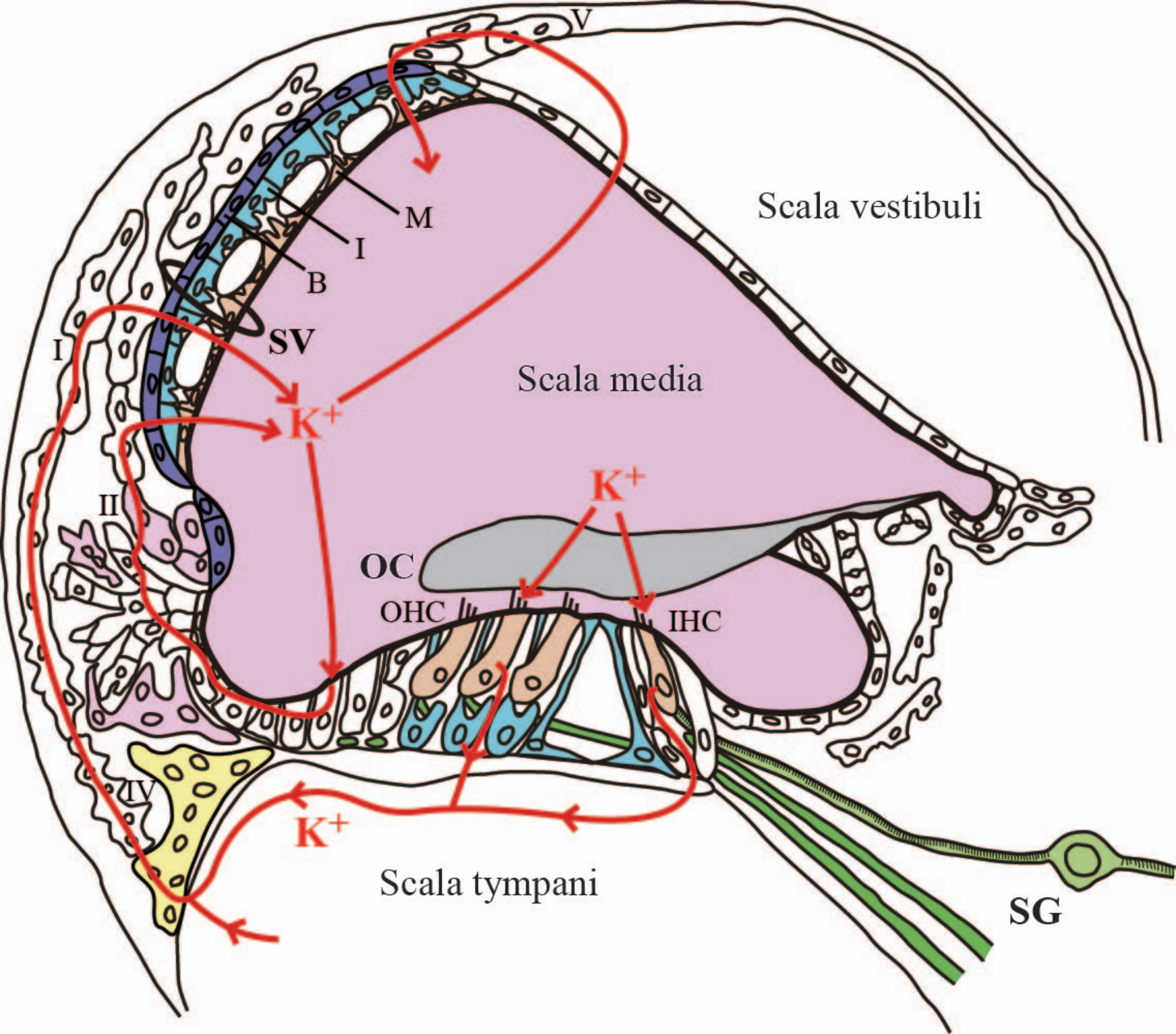
V
M
I
B
SV
I
Scala vestibuli
Scala media
K+
K+
II
OC
OHC
IHC
IV
K+
Scala tympani
SG

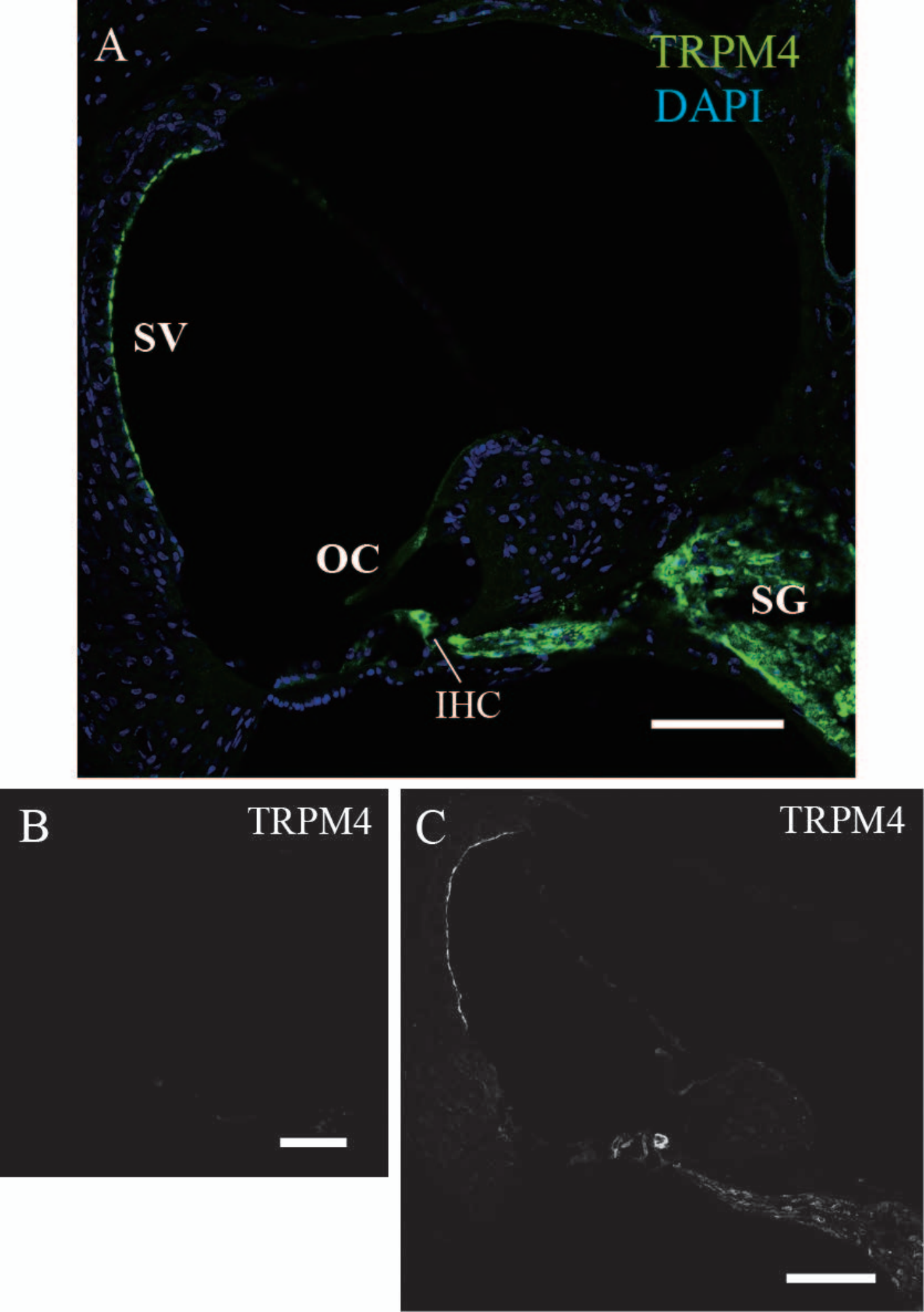
A
TRPM4
DAPI
SV
OC
SG
IHC
B
TRPM4
C
TRPM4

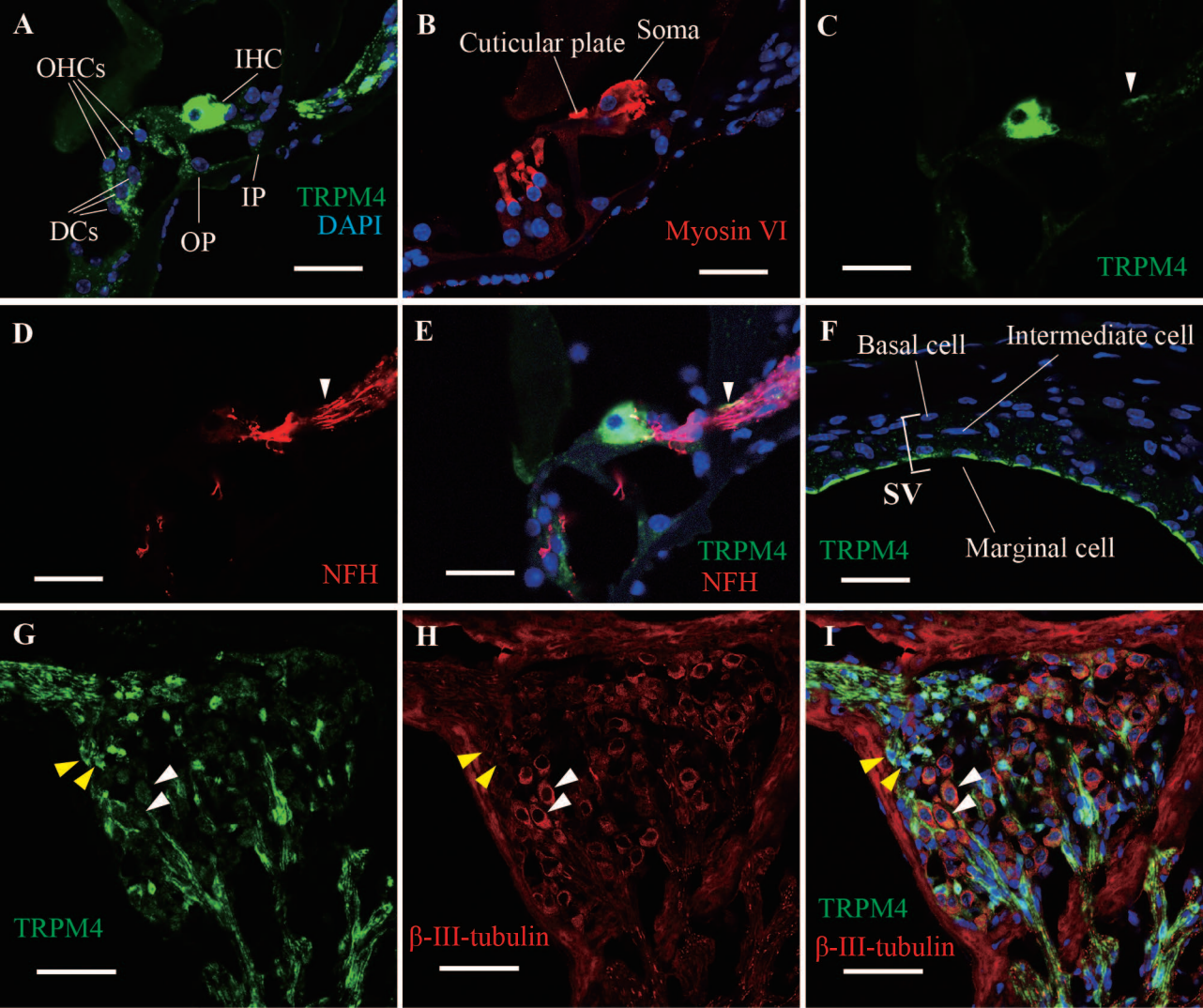
A
OHCs
IHC
IP
DCs
OP
TRPM4
DAPI
B
Cuticular plate
Soma
Myosin VI
C
TRPM4
D
NFH
E
TRPM4
NFH
F
Basal cell
Intermediate cell
SV
TRPM4
Marginal cell
G
TRPM4
H
β-III-tubulin
I
TRPM4
β-III-tubulin

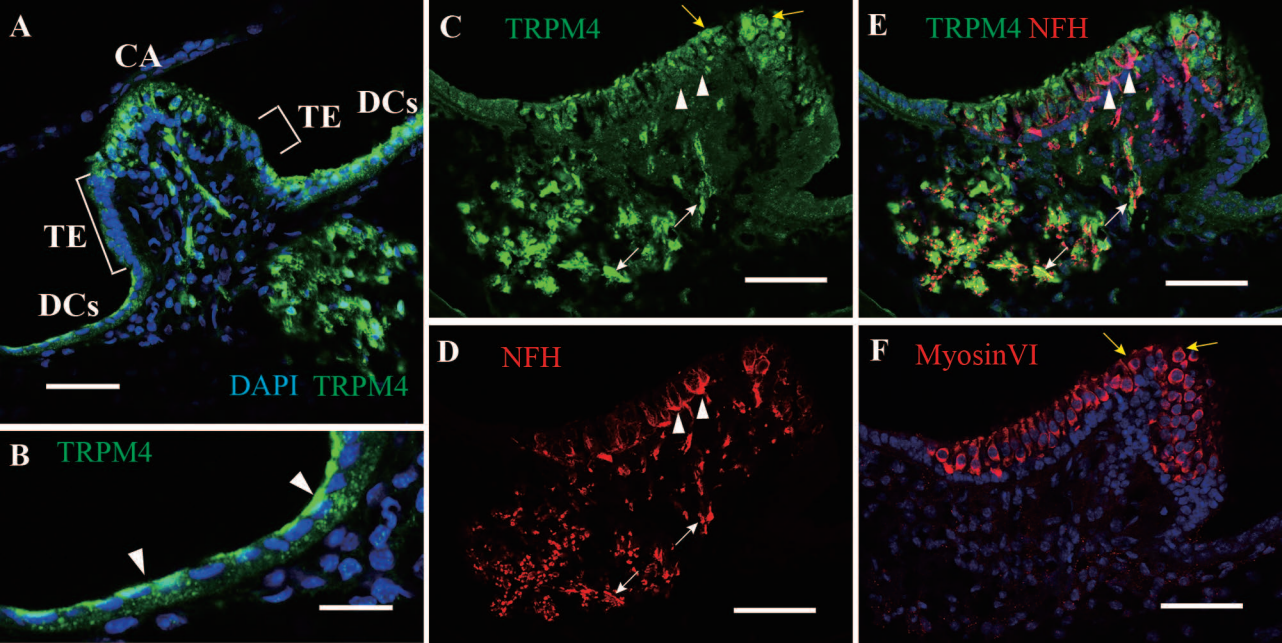
A
CA
TE
DCs
TE
DCs
DAPI TRPM4
B
TRPM4
C
TRPM4
D
NFH
E
TRPM4 NFH
F
MyosinVI

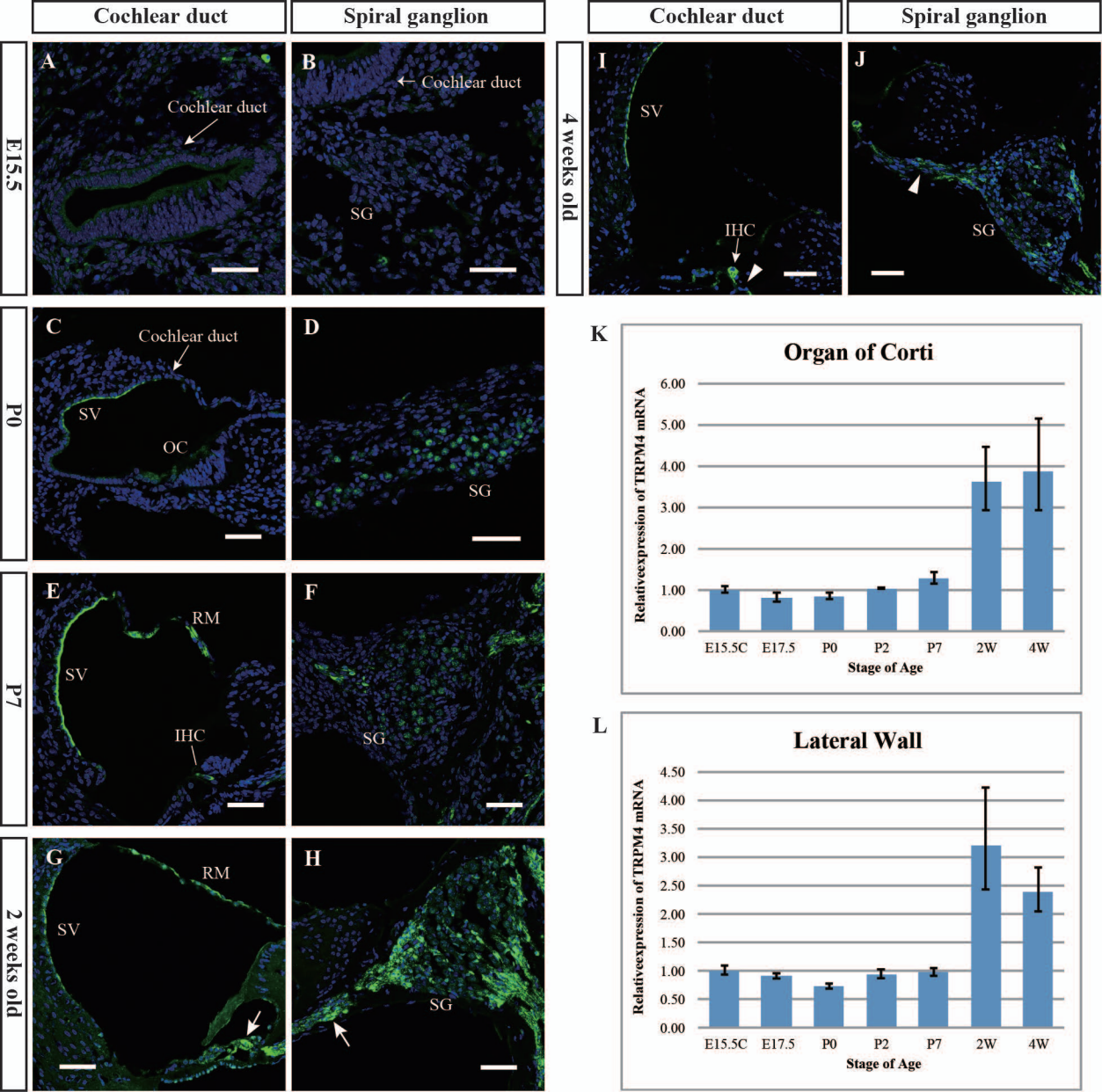
Cochlear duct
Spiral ganglion
Cochlear duct
Spiral ganglion
E15.5
4 weeks old
A
Cochlear duct
B
Cochlear duct
SG
I
SV
IHC
J
SG
P0
C
Cochlear duct
SV
OC
D
SG
K
Organ of Corti
Relativeexpression of TRPM4 mRNA
6.00
5.00
4.00
3.00
2.00
1.00
0.00
E15.5C
E17.5
P0
P2
P7
2W
4W
Stage of Age
P7
E
RM
SV
IHC
F
SG
L
Lateral Wall
Relativeexpression of TRPM4 mRNA
4.50
4.00
3.50
3.00
2.50
2.00
1.50
1.00
0.50
0.00
E15.5C
E17.5
P0
P2
P7
2W
4W
Stage of Age
2 weeks old
G
RM
SV
H
SG